ISSN 1070-3632, Russian Journal of General Chemistry, 2012, Vol. 82, No. 8, pp. 1342–1347. © Pleiades Publishing, Ltd., 2012.
Original Russian Text © L.V. Shapoval, V.V. Gorbunova, T.B. Boitsova, 2012, published in Zhurnal Obshchei Khimii, 2012, Vol. 82, No. 8, pp. 1252–1257.

Effect of Concentrations of Silver(I) and Gold(III) Initial Compounds on the Properties of AgAu Bimetal Nanocages

L. V. Shapoval, V. V. Gorbunova, and T. B. Boitsova

Herzen State Pedagogical University of Russia, Moyka emb. 48 , St. Petersburg, 191186 Russia
e-mail: tbboitsova@yandex.ru

Received February 16, 2012

Abstract—Results of studying kinetics of formation of hollow bimetal nanoparticles (nanocages) based on silver and gold that are obtained by the three-stage synthesis are presented. The factors defining sizes, structure, composition, and optical properties of nanocages were revealed by means of high-resolution transmission electron microscopy and energy-dispersive X-ray spectroscopy.

DOI: 10.1134/S1070363212080038

At present the attention of researchers is directed to the preparation and study of properties of the new type of bimetal nanostructures based on transition metals: nanocages [1], nanoframes [2], nanotori [3], etc. The interest to such structures is caused, first, by their high catalytic activity resulting from the extremely developed surface and selectivity reached by variation of the metal components ratio. For example, the catalytic activity of AuPd “nanorattles” in the reaction of *p*-nitrophenol transformation to *p*-aminophenol is eight times higher than that of monometallic gold “nanorattles” and four times compared to solid-gold nanoparticles [4]. Porous Pt and Pd nanowires synthesized earlier [5] are highly competitive with Pt and Pd on carbon catalysts in the catalytic activity in reactions of ethylene hydrogenation. Hollow and porous nanostructures show unique optical properties: the ability to selective absorption of light of certain wavelengths within the limits of visible and short-range IR region. It is fairly advantageous for the application of nanocages in photothermal therapy [6, 7] and photocatalysis [8]. For example, the photocatalytic decomposition of methyl orange [8] in the presence of AgAu nanocages proceeds more effectively than in the case of using traditional semiconductor catalysts like TiO_2 or ZnO. Bimetal AgAu nanostructures are also promising for the creation of substrates for surface-enhanced Raman scattering [9].

Properties of nanoparticles, including hollow particles, depend on size [10], therefore it is important for practical application that the method of their synthesis should provide certain size, size distribution, and stability of particles in aqueous solutions. The possibility of adjusting composition of nanoparticles is also of importance. The main way of obtaining hollow nanoparticles is galvanic substitution, the essence of which is presented in [11–14]. The formation of a nanoparticle is accompanied by a partial dissolution of the initial whole-metal particle and by a precipitation of a noble metal (gold, palladium, or platinum) layer, which protects a formed hollow particle from oxidation and makes it stable (resistant to dissolved oxygen) in aqueous solutions. However a spontaneous reaction of galvanic substitution excludes a possibility of control over the composition and the dispersity of the system.

The aim of the present work was to study the effect of concentrations of silver(I) and gold(III) compounds on the composition and the dispersity of nanocages obtained on their basis. The AgAu nanocages were prepared by the procedure of the three-stage synthesis developed earlier [15]. The procedure included: (a) the photochemical reduction of silver(I) ions from aqueous solutions of silver nitrate up to nanoparticles in the presence of poly-*N*-vinylpyrrolidone (PVP) as a stabilizer; (b) the reaction of galvanic substitution of gold for silver atoms; (c) the secondary photochemical reduction of intermediates [AgCl and silver(I) and gold(I) ions] up to metal forms.

The first stage is aimed at obtaining silver nanoparticles [15] functioning as template in the synthesis of nanocages. The photochemical reduction method promotes the formation of particles with regular icosahedron and decahedral shapes and a narrow size distribution. According to the transmission electron microscopy (TEM) data, the diameter of the particles was 33±3.3 nm.

In the second stage of the synthesis of AgAu nanocages a solution of hydrogen tetrachloroaurate(III) was added to the silver colloid prepared photochemically. As the standard electrode potential of the $AuCl_4^-/Au^0$ pair (0.99 V) is higher than that of the Ag^+/Ag^0 pair (0.8 V), the addition of $AuCl_4^-$ ions gives rise to the oxidation of silver nanoparticles [Eq. (1)].

$$3Ag^0_{particle} + AuCl^-_{4sol} \rightarrow Au^0_{particle} + 3Ag^+ + 4Cl^-_{sol}. \quad (1)$$

It follows from Eq. (1) that for the complete dissolution of a silver sample the reagents should be taken in the stoichiometric proportion 3:1 (3 silver atoms per 1 gold atom). Therefore, to obtain hollow bimetal structures, it is necessary to use $HAuCl_4$ in an amount less than equimolar. To analyze the effect of gold(III) ion concentration on the composition of resulting nanocages, we have selected a series of $HAuCl_4$ solutions with molar concentrations providing the following ratios of dispersed silver ions to gold(III) ions: (A) 5:1, (B) 4:1, and (C) 3:1.

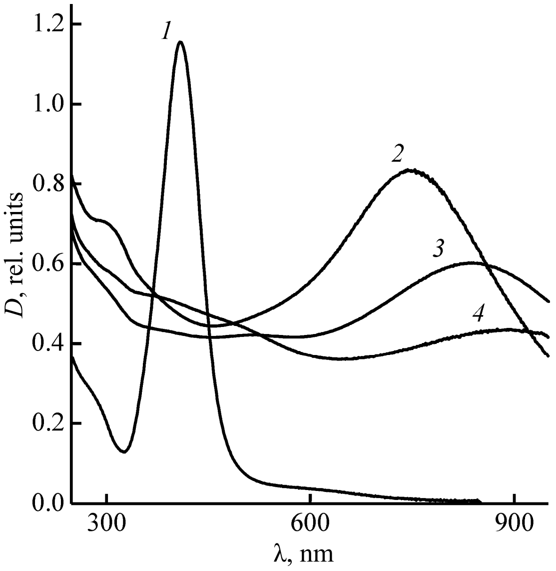

Fig. 1. Plasmon absorption spectra of (*1*) silver template and of bimetal nanocages obtained as a result of a galvanic substitution reaction at various molar ratios Ag and Au: (*2*) A; (*3*) B; (*4*) C.

Addition of a $HAuCl_4$ solution to a silver colloid results in lowering the intensity of the surface plasmon resonance (SPR) band at 414 nm and in its shift to the longwave spectral region (Fig. 1). Depending on the ratio of reagents, the SPR maximum reaches 754–890 nm (see the table). Color of the reaction mixture varies from green through brown to intensively dark blue. Using simple calculations [by Eq. (1)], we can expect that the reaction of galvanic substitution will result for sample A in the formation of bimetal nanocages with the Ag:Au = 2:1, for sample B, 1:1, and for sample C, of monometallic gold shells. These relations are realized on the condition that all gold ions have entered in a substitution reaction. However, by the results of high-resolution TEM, the diameter of internal hollows of nanocages was 25.4±3.5 nm, which is slightly less than the silver template size. Furthermore a metal → ligand charge transfer band of the initial compound $AuCl_4^-$ is observed at 300 nm in spectral curves of Fig. 1. An examination of optical density values in the region of 300 nm has shown that the content of $AuCl_4^-$ ions not involved in the substitution reaction decreases from 60 to 30% in the series of samples A, B, C. The scheme of reaction (1) does not exclude an intermediate formation of Au(I) ions [E^0 ($AuCl_4^-/AuCl_2^- + 2Cl^-$) 0.93 V] by Eq. (2).

$$AuCl^-_{2sol} + Ag^0_{particle} \rightarrow Au^0_{particle} + Ag^+_{sol} + 2Cl^-_{sol}. \quad (2)$$

Thus, even at a stoichiometric ratio of reagents the template is dissolved incompletely, which can be caused by a number of reasons: first, step-by-step consumption of Au(III) ions in the vicinity of Ag particles, therefore after a certain time the precipitation of gold changes to a diffusion mode; second, the

Spectral characteristics of bimetal AgAu nanocages with various Ag and Au molar ratios (samples A–C)

Sample	λ_{max} SPR, nm		λ_{min} SPR, nm		D_{max} SPR, rel. units		$\Delta\lambda_{max}$[a]
	before irradiation	after irradiation	before irradiation	after irradiation	before irradiation	after irradiation	
A	754	617	460	320	0.75	1.30	137
B	840	637	600	320	0.60	1.00	203
C	890	650	650	320	0.43	0.70	240

[a] $\Delta\lambda_{max}$ SPR = $\Delta\lambda_{max}$ SPR $_{before\ ir.}$ – $\Delta\lambda_{max}$ SPR $_{after\ ir.}$.

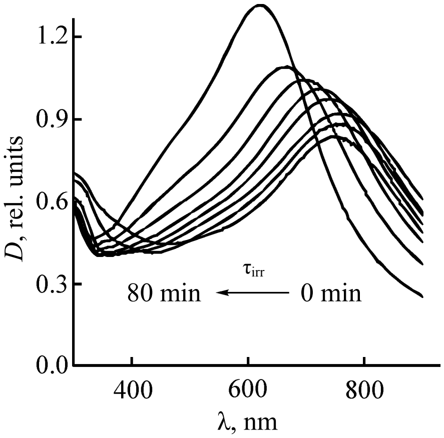

Fig. 2. Dynamics of the plasmon absorption spectrum of AgAu (A) bimetal colloid in the course of UV light irradiation within 80 min.

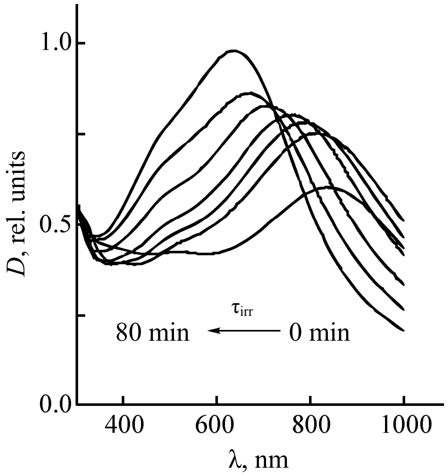

Fig. 3. Dynamics of the plasmon absorption spectrum of AgAu (B) bimetal colloid in the course of UV light irradiation within 80 min.

formation of intermediate Au(I) forms in the photolyte, which do not participate in the subsequent sorption on the surface of silver particles; and third, screening the surface of a silver particle with a gold layer, which leads to hampering diffusion of Ag(I) ions in a solution. Nevertheless, the observed dependence of the optical density variation in the maximum of SPR bands of nanocages on the Ag–$AuCl_4^-$ ratio is linear, which points to a proportional change of the silver/gold ratio in them (0.75, 0.60, and 0.43 for samples A, B, and C, respectively). These results suggest that AgAu bimetal nanocages are formed in the galvanic substitution stage.

To adjust the content of silver and gold in particles, in the third stage of the synthesis a photolysis was performed with the aim of reducing metal ions, which have passed in a solution as a result of a substitution reaction, and also of reducing AgCl. The irradiation of samples of the dispersion by UV light within 80 min is accompanied by the following spectral changes (Figs. 2–4): (a) a blue shift of the maximum of particles SPR up to 617, 637, and 650 nm for samples A, B, and C, respectively; (b) an increase in the intensity of SPR bands; (c) the appearance of a minimum in the region of 320 nm; (d) the formation of a shoulder at 516 nm, whose intensity and appearance time depend on the initial Au(III) concentration in the photolyte. The band at 516 nm dominates in the spectrum of sample C (Fig. 4).

Observations (a–d) can be assigned to the fact that silver(I) ions passed in a solution as a result of the galvanic substitution reaction are reduced on the surface of nanocages. By virtue of special features of silver optical characteristics [10] SPR bands of its particles are displaced to the short-wave region (380–500 nm), are highly intensive (surpass the intensity of bands of colloid gold of analogous concentration by two orders of magnitude), and have a minimum at 320 nm that makes it possible to identify them easily in the spectra of mixtures with gold particles. Alongside with it, the recorded position of SPR bands at wavelengths greater than 600 nm can testify in favor of hollow particles with the AgAu alloy structure [16], the content of silver in particles increasing in the series of samples A, B, and C, as follows from the value of blue shift of the SPR band maximum ($\Delta\lambda_{max}$ SPR, see the table).

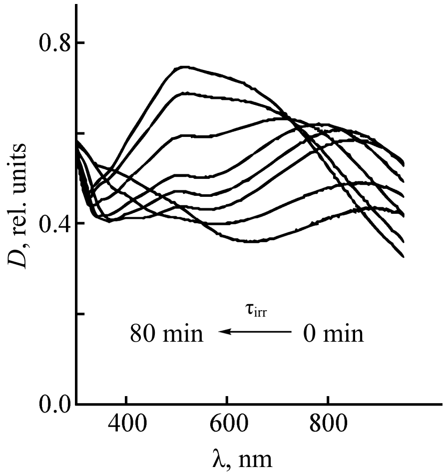

Fig. 4. Dynamics of the plasmon absorption spectrum of AgAu (C) bimetal colloid in the course of UV light irradiation within 80 min.

Appearance of a shoulder at 516 nm in the spectra is presumably caused by the fact that solid AgAu particles of a smaller size than the main fraction are formed in bulk photolyte. The gold component with an SPR band at 520 nm dominates in these particles [17]. The formation of metal particles of a smaller size can result from a fragmentation of hollow systems [13, 18] even at the galvanic substitution stage. Fragments of shells should bring a contribution to the absorption even in the prephotolysis stage, and bimetal colloids obtained after an irradiation should be characterized by a multimodal particle distribution. However bands characteristic for solid particles are absent from the absorption spectra of all samples (Fig. 1, curves *2*–*4*). The most probable reason for the appearance of a shoulder at 516 nm is the presence in the system of $AuCl_4^-$ ions in an amount, which decreases as the initial molar ratio [Ag]: [Au] decreases in the series of samples A–B–C. The necessity of participation of three electrons in the photolytic reduction of a complex predetermines the presumable formation of particles in the bulk photolyte.

Under the UV irradiation of $HAuCl_4$ both the formation of gold intermediate forms [Au(I) and $Au^0_{cluster}$] in bulk photolyte [Eqs. (3)–(5)] and their reoxidation by the initial gold(III) complex [Eq. (6)] can proceed simultaneously.

$$AuCl_4^- \xrightarrow{h\nu} (AuCl_4^-)^* \rightarrow AuCl_3^- + Cl, \tag{3}$$

$$2AuCl_3^- \rightarrow AuCl_2^- + AuCl_4^-, \tag{4}$$

$$3AuCl_2^- \xrightarrow{h\nu} AuCl_4^- + 2Au^0 + 2Cl^-, \tag{5}$$

$$3Au^0_{n\ \mathrm{cluster}} + AuCl^-_{4\ \mathrm{sol}} + 2Cl^- \rightarrow Au^0_{n-1\ \mathrm{cluster}} + 3AuCl^-_{2\ \mathrm{sol}}. \tag{6}$$

Last reaction (6) defines an induction period in the formation of gold particles, its duration increasing as the concentration of $AuCl_4^-$ ions in the photolyte increases.

Unlike photochemical reduction of gold(III), the reduction of silver(I) and gold(I) ions by reaction (5) involves only one electron, which results in a minimal induction period. Therefore UV irradiation of the systems results in the initial photoreduction on a surface of nanocages of silver(I) and gold(I) ions passed in a solution as a result of galvanic substitution, whereas the formation of gold particles from gold(III) ions occurs after the induction period, the duration of which decreases from 20 to 2 min in the series of samples A–B–C (Figs. 2–4). The position of the band at 516 nm, nevertheless, does not exclude a coreduction of silver(I) ions alongside with gold(III) ions.

Singular energy-dispersive X-ray spectral analysis has allowed us to determine the qualitative and quantitative composition of nanocages. Three represen-tative spectra of separate bimetal AgAu particles from samples with various initial ratios of Ag and Au atoms are presented in Fig. 5. In the spectra there are peaks of gold Mα (2.1 keV), Lα (9.7 keV), and Lβ (11.4 keV), and also characteristic peaks of silver Lα and Lβ at 2.9 and 3.15 keV, respectively, which confirms the presence of both metals in each separate particle. The quantitative analysis of synthesized nanoparticles for concentration of metals in atomic percents has shown the following ratios of silver and gold: 4:1 (A), 3:1 (B), and 2:1 (C). Deviation of these results from the theoretically expected values at the complete photo-reduction of ions (5:1; 4:1; 3:1) indirectly confirms the formation of solid metal particles in bulk photolyte. The important result of the analysis was the absence from the spectra of peaks characteristic of chlorine. According to the TEM data, the effective diameter of the synthesized AgAu nanocages (Fig. 6) is 37.0–39.5 nm.

The performed study has shown that the amount of silver and gold in bimetal nanocages depends on the initial ratio of concentrations of precursors and can be varied both in the stage of the galvanic substitution reaction and in the UV irradiation stage. The dispersity of samples is independent of the composition of nano-cells, which is promising for their practical application.

EXPERIMENTAL

The following reagents were used for the synthesis of silver-gold bimetal nanoparticles: hydrogen tetrachloaurate(III) trihydrate $HAuCl_4{\cdot}3H_2O$ (analytically pure grade, Acros organics, >99%; "P.L.Voikov Open Society Chemicals plant") and silver nitrate $AgNO_3$ (analytically pure grade Fisher Sci., > 99%; Reakhim). As a stabilizer of metal nanoparticles we applied PVP-40 (MM 40000, Sigma-Aldrich). The reagents in use were not exposed to additional refining. All solutions were prepared in deionized water (resistance of $18\times 10^6\ \Omega$ cm). Concentrations of compounds of metals were 5×10^{-4} M and that of PVP, 1.5%.

For irradiation we used monochromatic light of an RPR-100 photoreactor consisting of 15 mercury lamps, each of 35 W power, λ of excitation 254 nm, light flux intensity (by a ferrioxalate actinometer [20]) of

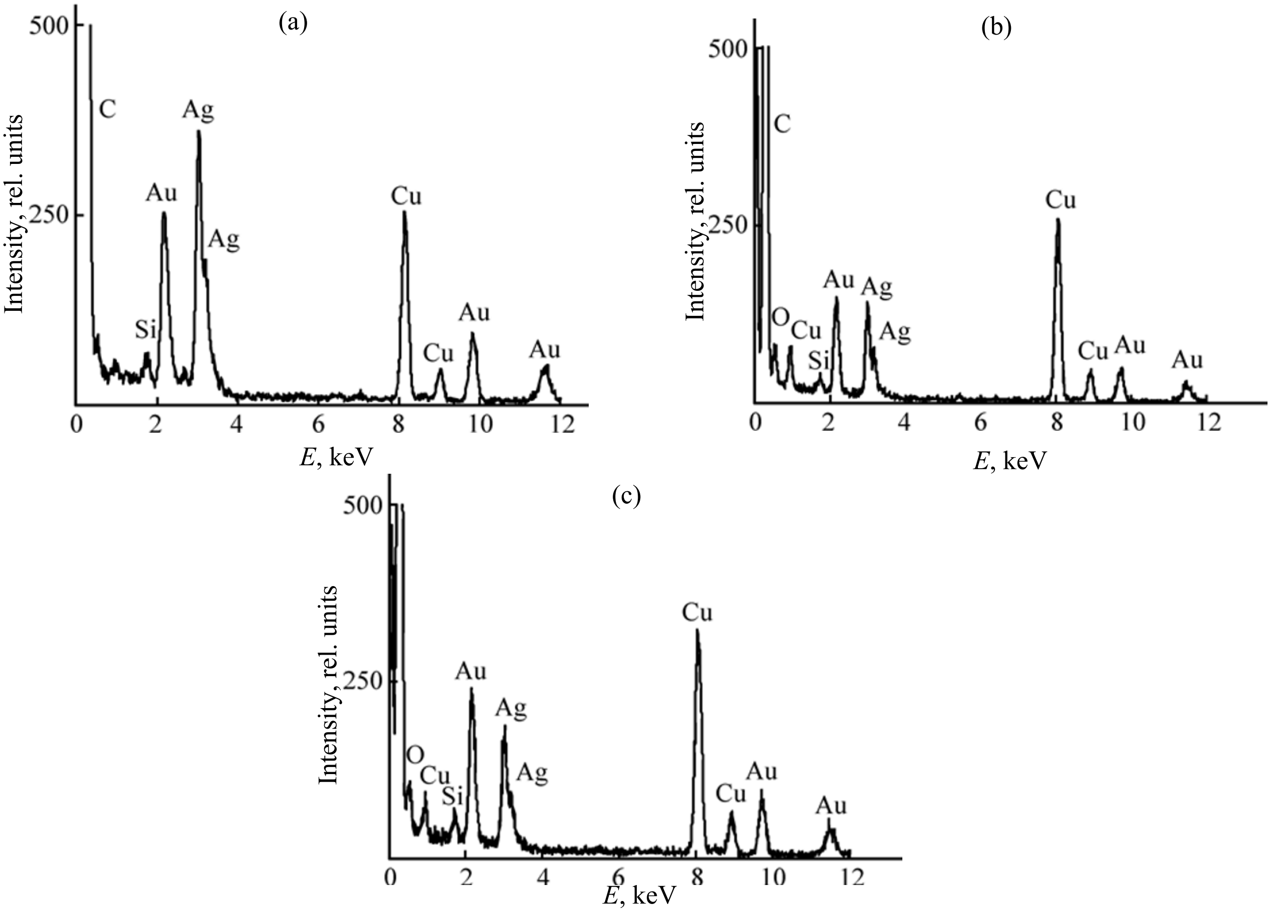

Fig. 5. Energy-dispersive X-ray spectra of separate samples of AgAu bimetal nanocages: A (a); B (b); C (c).

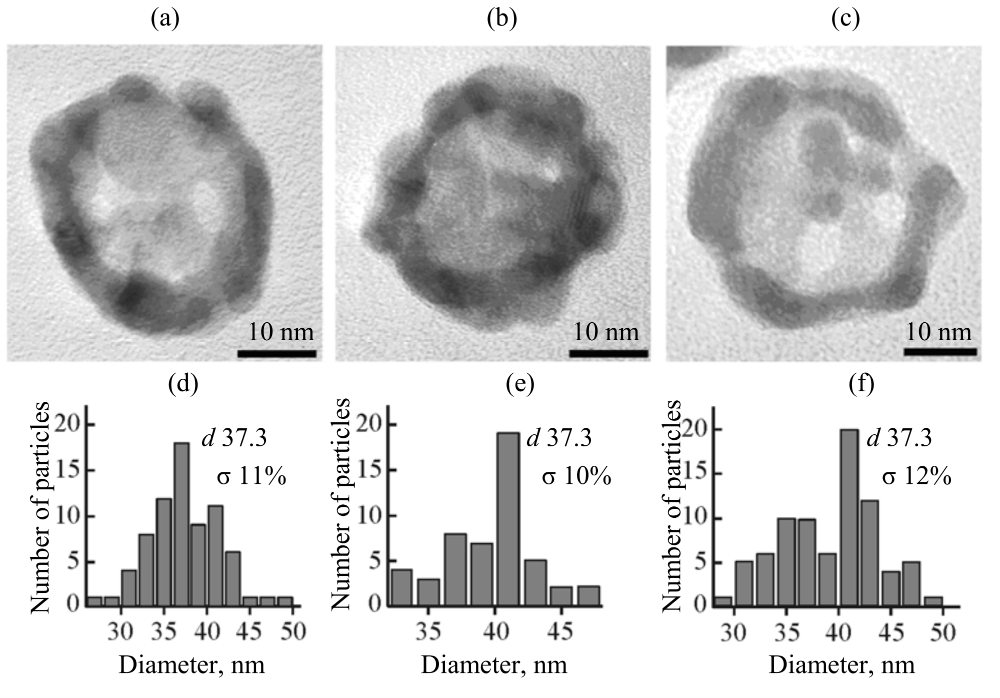

Fig. 6. Microphotographs of bimetal samples of AgAu nanocages: (a) A, (b) B, and (c) C and (d-f)the corresponding bar graphs.

1.7×10^{16} quantum/(cm^2 s). Directly before carrying out an experiment a photolyte was deaerated by passing through nitrogen. The irradiation was performed in quartz cells with optical path of length 5 mm. Absorption spectra of samples of colloids were recorded on a Varian Cary 50 Bio spectrophotometer over the range of 300–1000 nm in 0.2 nm steps of measuring. Elemental composition of prepared mono- and bimetal colloids was determined by the method of energy-dispersive X-ray structure analysis of separate nanoparticles, which was carried out in parallel with TEM using a Thermo Electron attachment and Noran System SIX software. Morphology of mono- and bimetallic nanoparticles was studied with the help of transmission electron microscopes Jeol SX-100 (accelerating voltage 100 kV) and Jeol JEM-2010 (accelerating voltage 200 kV). Samples for TEM were prepared by a four-fold centrifuging of colloids with separating a precipitate, their redispersing in methanol, subsequent depositing several drops of an alcohol dispersion on a copper net covered by a thin layer of amorphous carbon (200 mesh, Ted Pella, Inc., USA), and drying in air. Domination of energy lines of copper in the recorded spectra is caused by the nature of the substrate. An indistinct signal at 1.7 keV characteristic of silicon results from the fact that silicon is contained in the composition of greasing for rubber rings on a microscope holder, which leads to a negligible contamination of substrates with samples of nanoparticles.

ACKNOWLEDGMENTS

This work was financially supported by the grant of International Fulbright Graduate Program.

REFERENCES

1. Lu, X., Au, L., McLellan, J., Li, Z.-Y., Marquez, M., and Xia, Y., *Nano Lett.*, 2007, vol. 7, no. 6, p. 1764.
2. McEachran, M., Keogh, D., Pietrobon, B., Cathcart, N., Gourevich, I., Coombs, N., and Kitaev, V., *J. Am. Chem. Soc.*, 2011, vol. 133, no. 21, p. 8066.
3. Lu, X., Tuan, H.-Y., Chen, J., Li, Z.-Y., Korgel, B.A., and Xia, Y., *J. Am. Chem. Soc.*, 2007, vol. 129, no. 6, p. 1733.
4. Khalavka, Y., Becker, J., and Sonnichsen, C., *J. Am. Chem. Soc.*, 2009, vol. 131, no. 5, p. 1871.
5. Mohl, M., Kumar, A., Reddy, A., Kukovecz, A., Konya, Z., Kiricsi, I., Vajtai, R., and Ajayan, P.M., *J. Phys. Chem. (C)*, 2010, vol. 114, no. 1, p. 389.
6. Hu, M., Petrova, H., Chen, J., McLellan, J.M., Siekkinen, A.R., Marquez, M., Li, X., Xia, Y., and Hartland, G.V., *J. Phys. Chem. (B)*, 2006, vol. 110, no. 4, p. 1520.
7. Skrabalak, S.E., Chen, J., Sun, Y., Lu, X., Au, L., Cobley, C.M., and Xia, Y., *Accounts Chem. Res.*, 2008, vol. 41, no. 12, p. 1587.
8. Yen, C.W., Mahmoud, M.A., and El-Sayed, M.A., *J. Phys. Chem. (A)*, 2009, vol. 113, no. 16, p. 4340.
9. Feng, L., Gao, G., Huang, P., Wang, K., Wang, X., Luo, T., and Zhang, C., *Nano Biomed. Eng.*, 2010, vol. 2, no. 4, p. 258.
10. Bohren, C.F. and Huffman, D.R., *Absorption and Scattering of Light by Small Particles*, New York: Wiley, 1983.
11. Ramos, M., Ferrer, D.A., Chianelli, R.R., Correa, V., Serrano-Matos, J., and Flores, S., *J. Nanomaterials*, 2011, vol. 2011, p. 5.
12. Li, H., Ha, C.-S., and Kim, I., *J. Nanopart. Res.*, 2010, vol. 12, no. 3, p. 985.
13. Lu, X., Chen, J., Skrabalak, S.E., and Xia, Y., *Proc. IMechE. (N),* 2007, vol. 221, p. 1.
14. Teng, X., Wang, Q., Liu, P., Han, W., Frenkel, A.I., Marinkovic, N., Hanson, J.C., and Rodriguez, J.A., *J. Am. Chem. Soc.*, 2008, vol. 130, no. 3, p. 1093.
15. Shapoval, L.V., Gorbunova, V.V., and Boitsova, T.B., *Zh. Obshch. Khim.*, 2012, vol. 82, no. 8, p. 1277.
16. Prevo, B.G., Esakoff, S. A., Mikhailovsky, A., and Zasadzinski, J.A., *Small.*, 2008, vol. 4, no. 8, p. 1183.
17. Loginov, A.V., Boitsova, T.B., and Gorbunova, V.V., *J. Nanoparticle Res.*, 2002, vol. 4, no. 3, p. 193.
18. Sun, Y. and Xia, Y., *Nano Lett.*, 2003, vol. 3, no. 11, p. 1569.
19. Boitsova, T.B., Loginov, A.V., and Gorbunova, V.V., *Neorg. Mater.*, 1999, vol. 35, no. 12, p. 1449.
20. *Vvedenie v fotokhimiyu organicheskikh soedinenii* (Introduction to Photochemistry of Organic Compounds), Bekker, G.O., Ed., Leningrad: Khimiya, 1976, p. 145.